Milica Nikodijević Đorđević ✉
Jelena Petrović
Živojin Stamenković
Miloš Kocić
Dragiša Nikodijević

https://doi.org/10.21278/TOF.492071824
ISSN 1333-1124
eISSN 1849-1391

IMPACT OF ELECTRICAL AND MOVING MAGNETIC FIELDS ON THE HEAT TRANSFER FLOW OF IMMISCIBLE PURE FLUIDS AND NANOFLUIDS THROUGH POROUS MEDIA WITH VARIED POROSITY

Summary

This paper discusses fully developed electromagnetohydrodynamic (EMHD) flow and heat transfer of an immiscible pure fluid and a nanofluid in a horizontal channel. The channel is saturated with a porous medium, and its top and bottom halves have different porosities. The pure fluid flows through the top half, while the nanofluid flows through the bottom half. Impermeable isothermal horizontal plates act as the channel walls. The channel is influenced by an external moving homogeneous magnetic field. Analytical distributions of fluid flow velocity and fluid temperature in the channel as a function of the physical parameters are introduced specifically to address this problem. The distributions are also presented as graphs for multiple values of the introduced parameters. The Nusselt number and skin friction values on the channel walls are also determined and presented in a table. The analysis of the obtained results is followed by the resulting conclusions about the impact of introduced parameters on the fluid flow and heat transfer in the observed channel.

Key words: *heat transfer, nanofluid, electric field, moving magnetic field, porous medium, Nusselt number*

1. Introduction

Convective heat transfer is ubiquitous in nature and has numerous practical applications ranging from multiple industries to biomedicine. Accordingly, many studies have been conducted to improve convective heat transfer using porous media, electric fields, magnetic fields, and so on. The presentation and subsequent publication of the study by Choi [1] initiated extensive research into nanofluids for the purpose of improving heat convection. The idea had been introduced by Maxwell [2] as early as 1873, but owing to insufficiently developed technology at the time, such undertakings were not feasible. Even to this day, contradictory conclusions may still be found among nanofluid studies, but there are also numerous indisputable conclusions that address the advantages of nanofluids over classical fluids used for heat transfer, as corroborated by Goncalves et al. [3] and Hamad et al. [4].

The studies on this topic continued to grow in number. Nikodijević et al. [5] studied the magnetohydrodynamic (MHD) flow and heat transfer of two immiscible fluids in a horizontal channel through a porous medium with different porosities. The channel walls were isothermal, with a moving upper wall and an externally applied magnetic field inclined in relation to the channel. Das et al. [6] investigated a fully developed mixed convective nanofluid flow in a vertical channel influenced by a homogeneous transversal magnetic field. They also considered an induced magnetic field. Lima et al. [7] explored the MHD flow and heat transfer of two immiscible fluids in an inclined channel between parallel plates. They considered the effects of porous layers, buoyancy, Joule and viscous heating, moving plates, inclined magnetic fields, and heat generation/absorption. Petrović et al. [8] studied the flow and heat transfer of two immiscible fluids in a horizontal channel through a porous medium with different porosities. The fluids were influenced by an external electric field and an external inclined magnetic field. Analytical distributions of fluid velocity and temperature were determined. Seth et al. [9] investigated the effects of viscous and ohmic heating and heat generation/absorption on the MHD flow of a thin Casson fluid film over a horizontal stretching sheet in a non-Darcy porous medium. They determined velocity and temperature distributions, the local friction coefficient, and the local Nusselt number. Dogonchi et al. [10] explored the natural convective heat flow of a nanofluid in a channel between a hot rectangular cylinder and a cold circular cylinder influenced by an external inclined homogeneous magnetic field. The channel was saturated with a porous medium for which the Brinkman model was used. Prasad et al. [11] studied the fluid flow and heat transfer in a vertical double passage channel with applied electric and magnetic fields using the Robin boundary conditions. They determined the analytical solutions using the regular perturbation method and the differential transform method. Manjet and Sharma [12] investigated the flow and heat convection of two immiscible fluids – a Newtonian fluid and a nanofluid – in a horizontal channel. They examined the effects of different physical parameters on the velocity and temperature, the Nusselt number, and the skin friction coefficient. Umavathi and Chamkha [13] developed a new mathematical model for natural nanofluid convection in a vertical channel with the effects of thermo-solutal convection and cross diffusions using Fourier-type conditions. Nikodijević et al. [14] explored the unsteady MHD flow and heat transfer in a horizontal channel through a porous medium. The channel walls were isothermal and impermeable, and the applied magnetic field was inclined in relation to the horizontal channel walls. Umavathi and Sheremet [15] studied the convective heat transfer of three immiscible fluids in a vertical channel. The middle layer contained a clear viscous fluid, while the left and right layers contained nanofluids. The nanofluids flowed through porous media, and they were examined using the Darcy model. Mahabaleshwar et al. [16] investigated the MHD flow of a hybrid nanofluid and mass transfer along a horizontal sheet stretching at square velocity through a porous medium. Raje et al. [17] explored the axis-symmetrical flow and heat transfer of two immiscible fluids in a circular tube. The tube core contained a micropolar fluid, while the peripheral portions contained a Newtonian fluid. Two cases were considered: one with a complete non-porous fluid region and another with the peripheral portion of the circular tube saturated with a porous medium. Das et al. [18] studied the unsteady MHD flow and heat transfer of an ethylene glycol-silver nanofluid in a vertical channel. The channel walls were permeable, and the channel was saturated with a porous medium. Heat radiation and Hall currents were taken into account. Raje and Bhise [19] investigated the unsteady MHD flow and heat transfer of three immiscible fluids in a horizontal channel whose central portion contained a Casson fluid, while the peripheral portions contained Newtonian fluids. The channel was saturated with a porous medium. Umavathi et al. [20] explored the high-temperature unsteady MHD flow of a Casson nanofluid between parallel permeable discs with Fourier-type boundary conditions, including

radiation. Raju and Rao [21] studied the effect of Hall current on unsteady MHD flow and heat transfer of two immiscible fluids in a horizontal channel between parallel conductive plates. The channel was placed in a rotating frame. Prasad et al. [22] investigated the fully developed MHD flow and heat transfer of water-based nanofluids in a vertical double passage channel. They used the perturbation method and the differential transform method. Raju and Rao [23] explored the effect of the Hall current and the Coriolis force on unsteady electromagnetohydrodynamic (EMHD) flow of two immiscible fluids and heat transfer in a horizontal channel between parallel non-conductive plates. Soomro et al. [24] studied the MHD flow and heat transfer of a hybrid Al_2O_3–Cu/H_2O nanofluid along an inclined stretching plate. A magnetic field was applied perpendicular to the plate. Yadav et al. [25] investigated the effect of magnetic field on entropy generation, fluid velocity, microrotation, and temperature of two immiscible fluids in a channel. One fluid was micropolar, and the other was a Newtonian fluid. The channel walls were isothermal, and the channel was saturated with two different porous media. Rikitu et al. [26] explored the unsteady mixed convection flow and heat transfer via radiation of nanofluids with variable transfer properties in a microchannel through a porous medium. They used convective boundary conditions. Siva et al. [27] studied the unsteady EMHD flow of a non-Newtonian fluid in a microchannel. A voltage coupling model was used for the non-Newtonian fluid. Alzahrani et al. [28] investigated the effects of a chemical reaction and rotation on EMHD flow and heat transfer of two immiscible fluids in a horizontal channel between parallel rotating plates. One fluid was Newtonian, and the other was a Casson fluid. The plates were isothermal and electrically insulated. An external electric field and an external inclined magnetic field were applied to the channel. Hussain et al. [29] explored the MHD dissipation, heat absorption, chemical reaction, and radiation during the nanofluid flow over a stretchable surface, together with the heat and mass transfer. Numerical calculations were based on three water-based nanofluids with titanium oxide, aluminium oxide, and copper nanoparticles. Petrović et al. [30] studied the fully developed EMHD flow and heat transfer in a horizontal channel between parallel isothermal impermeable plates. The channel was saturated with different porous media. A nanofluid flows through the bottom portion of the channel, while a clear fluid flows through the top portion, with the fluids being immiscible.

Nabwey et al. [31] gave an overview of significant research for the period 2018-2020 on the MHD flow of nanofluids in a porous medium in order to improve heat transfer. At the end they suggested directions for further research. The influence of EMHD effects on the flow and heat transfer of nanofluids in a porous inclined medium between clear fluids was investigated by Subray et al. [32]. Kalyan and Soliman [33] investigated the interaction of electrical conductivity, natural convection, micropolar effect and chemical reaction in immiscible fluids in a vertical channel. Rao and Deka [34] investigated the MHD flow and heat transfer of a hybrid nanofluid in a porous medium. Boundary conditions are first-order slip conditions.

The authors of the present paper reviewed a copious number of available studies concerning the MHD flow and heat transfer, porous media, and nanofluids. The overview revealed that there are not many studies analysing the flow of immiscible fluids, especially if one of the fluids is a nanofluid, which has also been observed by other authors, for instance, Umavathi and Sheremet [15]. No study was found to analyse the impact of an applied moving magnetic field on fluid flow and heat transfer. Such observations were what motivated the present study to focus on the flow and heat transfer in a horizontal channel between parallel walls of two immiscible fluids, one being a clear fluid and the other a nanofluid. The channel is saturated with porous media of different porosities, and its walls are isothermal, impermeable, and electrically insulated. The channel is under the influence of an external homogeneous electric field and an external homogeneous moving magnetic field. The investigation of the impact of a moving magnetic field on fluid flow and heat transfer is a

novel contribution of this paper. It is expected that the results will be useful for further research, particularly for the design of precision biomedical recording instruments in order to improve patients' safety during such recordings.

2. Mathematical formulation

The paper considers the fully developed (EMHD) flow and heat transfer of two immiscible fluids in a horizontal channel between two parallel plates, which are fixed, impermeable, electrically insulated, and isothermal. The top and bottom plates are at constant temperatures, Tw_1 and Tw_2, respectively. The channel is saturated with different porous media. The permeability of the top half of the channel is K_1, while the permeability of the bottom half is K_2. A clear fluid flows through the top portion, and a nanofluid flows through the bottom portion. The channel is under the influence of an external homogeneous electric field perpendicular to the longitudinal vertical plane of the channel and an external homogeneous magnetic field perpendicular to the plates. The external magnetic field moves at constant velocity U_0 in the direction of primary flow. For the selected coordinate system (Fig. 1), electric field E moves along the z-axis, magnetic field B along the y-axis, while the magnetic field velocity is directed along the x-axis. The pressure gradient along the x-axis is considered to be constant, as are the physical properties of both fluids.

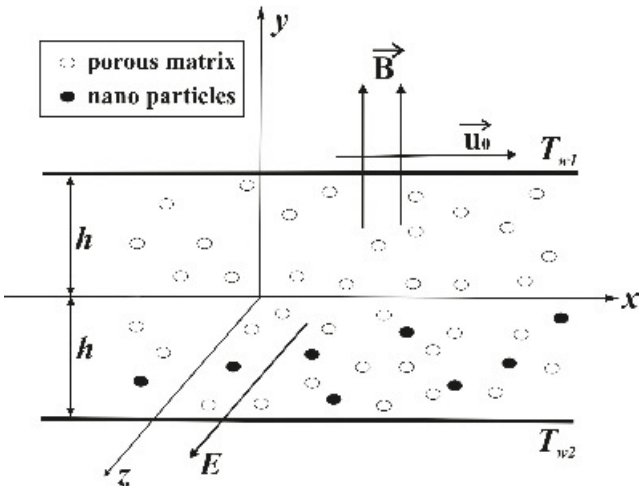

Fig. 1 Physical model

The mathematical model of the described fluid flow and heat transfer is represented by the following impulse and energy equations [30, 35]:

$$-\frac{\partial p}{\partial X}+\mu_j\frac{\mathrm{d}^2U_i}{\mathrm{d}Y^2}-\frac{\mu_j}{K_i}U_i-B\sigma_j\left[E+B\left(U_i-U_0\right)\right]=0 \tag{1}$$

$$k_j\frac{\mathrm{d}^2T_i}{\mathrm{d}Y^2}+\mu_j\left(\frac{\mathrm{d}U_i}{\mathrm{d}Y}\right)^2+\frac{\mu_j}{K_i}U_i^2+\sigma_j\left[E+B\left(U_i-U_0\right)\right]^2=0 \tag{2}$$

with the corresponding boundary conditions and interface conditions in the following form:

$$\begin{aligned}&\left(U_1,T_1\right)(h)=\left(0,T_{w1}\right),\left(U_2,T_2\right)(-h)=\left(0,T_{w2}\right),\\&\left(U_1=U_2,T_1=T_2,\mu_1\frac{\mathrm{d}U_1}{\mathrm{d}Y}=\mu_{nf}\frac{\mathrm{d}U_2}{\mathrm{d}Y},k_1\frac{\mathrm{d}T_1}{\mathrm{d}Y}=k_{nf}\frac{\mathrm{d}T_2}{\mathrm{d}Y}\right)(0).\end{aligned} \tag{3}$$

Hereinafter, the subscripts *i* and *j* have the following values: *i*=1, *j*=1 for region 1, and *i*=2, *j*=*nf* for region 2.

Classical expressions are used for the physical properties of the nanofluid in the following form:

$$\mu_{nf}=\frac{\mu_f}{(1-\phi)^{2.5}},\ k_{nf}=X(k)k_f,\ \sigma_{nf}=X(\sigma)\sigma_f,\quad X(\zeta)=\frac{\zeta_S+2\zeta_f-2\phi(\zeta_f-\zeta_S)}{\zeta_S+2\zeta_f+\phi(\zeta_f-\zeta_S)} \tag{4}$$

where subscripts *f*, *s*, and *nf* denote the physical properties of the base fluid, the nanoparticles, and the nanofluid, respectively. The symbol ϕ is the volume fraction of nanoparticles.

To facilitate further analysis, it is more convenient to transform equations (1) and (2) and conditions (3) into their dimensionless forms, for the purpose of which the following dimensionless quantities are introduced:

$$y=\frac{Y}{h},\ u_i=\frac{U_i}{U},\ \theta_i=\frac{T_i-T_{w2}}{T_{w1}-T_{w2}} \tag{5}$$

where *U* is the characteristic velocity that will be determined later.

Application of the introduced dimensionless quantities (5) yields the following dimensionless forms of equations (1) and (2):

$$\frac{\mathrm{d}^2u_i}{\mathrm{d}y^2}-\omega_i^2u_i=G_i, \tag{6}$$

$$\frac{\mathrm{d}^2\theta_i}{\mathrm{d}y^2}+b_iB_r\left[\left(\frac{\mathrm{d}u_i}{\mathrm{d}y}\right)^2+\omega_i^2u_i^2+S_iu_i+L_i\right]=0, \tag{7}$$

respectively, where the introduced notations are expressed as:

$$\omega_i^2=\Lambda_i+\frac{m_i}{n_i}Ha^2,\ G_i=m_i\left(\frac{Q}{n_i}Ha^2-P_1\right),\ Q=K-\delta,\ S_i=2\frac{m_i}{n_i}QHa^2,$$
$$L_i=\frac{1}{2}QS_i,\ m_i=\frac{\mu_1}{\mu_j},\ n_i=\frac{\sigma_1}{\sigma_j},\ q_i=\frac{k_1}{k_j},\ b_i=\frac{q_i}{m_i},\ m=m_2,\ q=q_2,\ B_r=\frac{\mu_1U^2}{k_1(T_{w_1}-T_{w_2})}; \tag{8}$$
$$P_1=P\frac{h^2}{U\mu_1},\ Ha^2=B^2h^2\frac{\sigma_1}{\mu_1},\ \Lambda_i=\frac{h^2}{K_i},\ K=\frac{E}{BU},\ \delta=\frac{U_0}{U},\ P=-\frac{\partial p}{\partial X}.$$

The dimensionless form of conditions (3) is written as:

$$(u_1,\theta_1)(1)=(0,1),\ (u_2,\theta_2)(-1)=(0,0),$$
$$\left(u_1=u_2,\ \theta_1=\theta_2,\ m\frac{\mathrm{d}u_1}{\mathrm{d}y}=\frac{\mathrm{d}u_2}{\mathrm{d}y},\ q\frac{\mathrm{d}\theta_1}{\mathrm{d}y}=\frac{\mathrm{d}\theta_2}{\mathrm{d}y}\right)(0). \tag{9}$$

The next step is to analyse the dimensionless mathematical model of the described problem, i.e., equations (6) and (7) with conditions (9).

3. Solutions

Equations (6) and (7) are regular differential equations, so their solutions can be determined directly. The solution of equation (6) can be represented as

$$u_i(y)=C_i\exp(\omega_iy)+D_i\exp(-\omega_iy)+A_i, \tag{10}$$

and the solution of equation (7) as

$$\theta_i(y) = -b_i B_r \left\{ \frac{1}{2}\left[C_i^2 \exp(2\omega_i y) + D_i^2 \exp(-2\omega_i y) \right] + \frac{M_i}{\omega_i^2}\left[C_i \exp(\omega_i y) + D_i \exp(-\omega_i y) \right] + \frac{1}{2} N_i y^2 + E_i y + F_i \right\}. \tag{11}$$

The integration constants C_1, C_2, D_1, D_2, F_1, F_2, E_1, and E_2, determined using conditions (9), and the notations introduced for the purpose of brevity are given below:

$$\begin{aligned}
&C_1 = \frac{R_4 R_5 - R_3 R_6}{R_1 R_5 - R_2 R_3},\ C_2 = \frac{1}{R_3}(R_1 C_1 - R_4),\ D_1 = -C_1 \exp(2\omega_1) - A_1 \exp(\omega_1),\\
&D_2 = -C_2 \exp(-2\omega_2) - A_2 \exp(-\omega_2),\ F_1 = b_2 F_2 + R_9,\ E_1 = R_7 - R_9 - b_2 F_2,\ E_2 = F_2 - R_8,\\
&F_2 = \frac{m(R_7 - R_9) + R_8 - R_{10}}{1+q},\ A_i = -\frac{G_i}{\omega_i^2},\ M_i = 2A_i\omega_i^2 + S_i,\ N_i = \omega_i^2 A_i^2 + S_i A_i + L_i,\\
&R_1 = 1 - \exp(2\omega_1),\ R_2 = m\omega_1\left[1 + \exp(2\omega_1)\right],\ R_3 = 1 - \exp(-2\omega_2),\\
&R_4 = A_2\left[1 - \exp(-\omega_2)\right] - A_1\left[1 - \exp(\omega_1)\right],\ R_5 = \omega_2\left[1 + \exp(-2\omega_2)\right],\\
&R_6 = \omega_2 A_2 \exp(-\omega_2) - m\omega_1 A_1 \exp(\omega_1),\ \Omega(i,t) = -\frac{1}{2}\left[C_i^2 \exp(-2t\omega_i) + D_i^2 \exp(2t\omega_i) \right] -\\
&\frac{M_i}{\omega_i^2}\left[C_i \exp(-t\omega_i) + D_i \exp(t\omega_i) \right] - \frac{1}{2} N_i,\ R_7 = \Omega(1,-1) - \frac{1}{Br},\ R_8 = \Omega(2,1),\\
&\psi(i) = \frac{1}{2}\omega_i\left(C_i^2 + D_i^2\right) + \frac{M_i}{\omega_i^2}(C_i + D_i),\ R_9 = b_2\psi(2) - \psi(1),\\
&Z(i) = \omega_i\left(C_i^2 - D_i^2\right) + \frac{M_i}{\omega_i}(C_i - D_i),\ R_{10} = Z(2) - mZ(1).
\end{aligned} \tag{12}$$

Skin friction in its dimensionless form and the Nusselt number are written as:

$$\tau_i = \frac{\mu_j}{\mu_1}\frac{\mathrm{d}u_i}{\mathrm{d}y},\ Nu_i = \frac{k_j}{k_1}\frac{\mathrm{d}u_i}{\mathrm{d}y}. \tag{13}$$

Dimensionless skin frictions on the top and bottom plates are written in the following forms, respectively:

$$\tau_1 = Q(1,1),\ \tau_2 = \frac{1}{m}Q(2,-1),\ Q(i,t) = \omega_i\left[C_i \exp(t\omega_i) - D_i \exp(-t\omega_i) \right], \tag{14}$$

while the Nusselt number on the top and bottom plates is expressed as

$$\begin{aligned}
&Nu_1 = S(1,1),\ Nu_2 = \frac{1}{m}S(2,-1),\\
&S(i,t) = Br\left\{\omega_i\left[C_i^2 \exp(2t\omega_i) - D_i^2 \exp(-2t\omega_i) \right] + \right.\\
&\left.\frac{M_i}{\omega_i}\left[C_i \exp(2t\omega_i) - D_i \exp(-t\omega_i) \right] + tN_i + F_i \right\},
\end{aligned} \tag{15}$$

respectively.

4. Verification, results, and analysis

The first step in this section is the verification of the model used in the study. To this end, the results presented in Malashetty et al. [37] are used when the channel inclination angle is equal to zero, i.e., when the channel is horizontal, and the external power factor is K=–1.

This case is a part of the set of cases considered in this study for the following values of physical parameters: velocity ratio (δ=0), volume fraction of nanoparticles (ϕ=0), thermal conductivity ratio (k=1), dynamic viscosity ratio (m=0.5), electrical conductivity ratio (n=0.5), Hartmann number (Ha=2), porosity factor of medium 1 (Λ_1=0), porosity factor of medium 2 (Λ_2=0), dimensionless pressure gradient (P_1=5), and external electrical load factor (K=–1). The velocity distributions for this case obtained in the present study and in Malashetty et al. [37] are shown in Fig. 2. The velocity distributions have a good degree of overlap, with a maximum deviation of less than 2%, which is satisfactory considering that the results in [37] were shown as diagrams and that the authors used the approximate perturbation method.

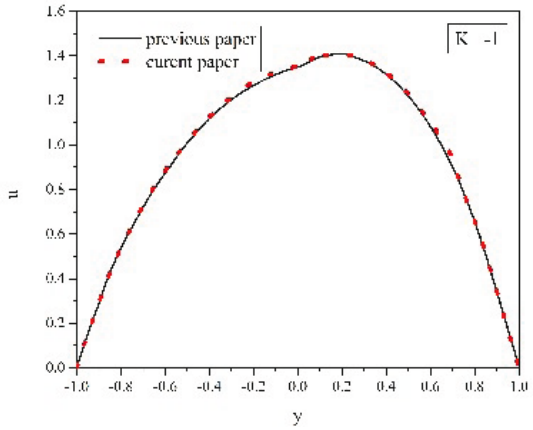

Fig. 2 Velocity comparison between Malashetty et al. [37] and the current study

This section presents a portion of the obtained results for the case when oil flows through channel region 1 and copper-water nanofluid through channel region 2. The utilized physical properties, i.e., density (ρ), specific heat capacity (c_p), thermal conductivity (k), electrical conductivity (σ), and dynamic viscosity (μ), for oil, water, and copper are given in Table 1. The results are given for P_1=1, as proposed by Lohrasbi and Sahani [36], although other values may be used, for example, in Malashetty et al. [37]. This automatically means that characteristic velocity is selected in the form:

$$U = -\frac{h^2}{\mu_1}\frac{\partial p}{\partial X}. \tag{16}$$

For clarity and ease of analysis, the results are shown in Figures 3-12 and in Table 2 for several values of the introduced physical parameters.

Table 1 Physical properties of water, oil, and copper

Physical properties	ρ (kg/m^3)	c_p (J/(kgK))	k (W/(Km))	σ (S/m)	μ (Pas)
Water	997.1	4179	0.613	$5.5\cdot10^{-6}$	0.01
Oil	900	1800	0.15	$3\cdot10^{-7}$	0.5
Copper	8933	385	401	$59.6\cdot10^{6}$	-

Thus, Figs. 3 and 4 show the distributions of dimensionless velocity and temperature, respectively, for different Hartmann number values. Figure 3 shows that higher Ha values correspond to higher fluid velocities in region 1 and lower velocities in region 2.

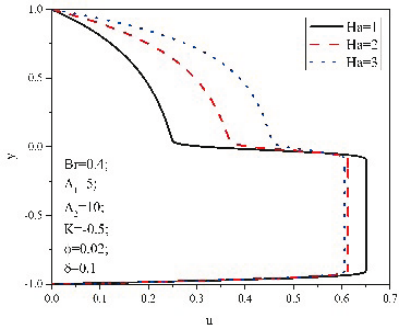

Fig. 3 Velocity distributions for different Hartmann numbers (Ha)

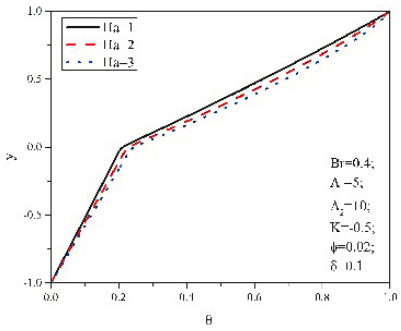

Fig. 4 Temperature distributions for different Hartmann numbers (Ha)

Velocities in region 2 are higher than those in region 1 because the influence of viscous force is much higher in region 1. Figure 4 shows that higher Hartmann numbers correspond to higher fluid temperatures. Heat transfer in region 2 is usually conductive. On the top plate, for Ha values of 2 and 3, heat is transferred from the fluid to the plate, whereas for an Ha value of 1, heat is transferred from the plate to the fluid.

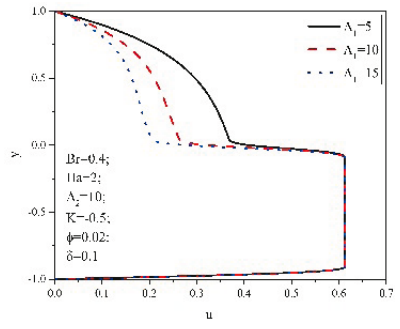

Fig. 5 Velocity distributions for different porosity factors (Λ_1)

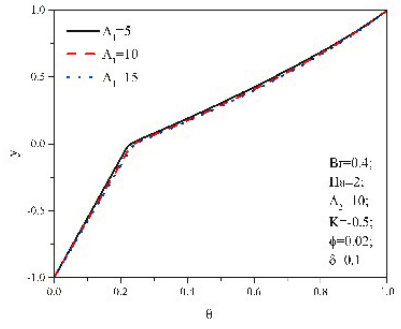

Fig. 6 Temperature distributions for different porosity factors (Λ_1)

Figures 5 and 6 show dimensionless velocity and temperature distributions, respectively, for different porosity factors in region 1 and constant porosity factors in region 2. It is noticeable that increased porosity factors reduce the velocity and increase the temperature. Higher porosity factors correspond to less permeable media in region 1, which in turn increases the Darcy flow resistance and decreases velocity. Region 2 velocity remains almost exactly the same because the porosity factor of this medium is constant. Overcoming this force requires additional energy, which is transformed into heat, causing a temperature increase.

Figures 7 and 8 show dimensionless velocity and temperature distributions for different nanoparticle volume fractions, respectively. Increased nanoparticle volume fraction increases

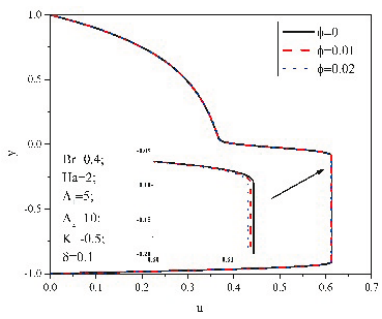

Fig. 7 Velocity distributions for different nanoparticle volume fractions (ϕ)

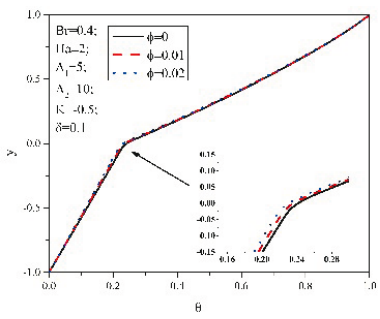

Fig. 8 Temperature distributions for different nanoparticle volume fractions (ϕ)

the concentration of copper nanoparticles in the base fluid/water, which leads to increased density, dynamic viscosity coefficient, thermal conductivity, and electrical conductivity of the nanofluid. Higher density and dynamic viscosity of the nanofluid decelerate the nanofluid flow in region 2, whereas the velocity changes in region 1 are almost imperceptible and are solely due to velocity continuity conditions at the interface, as shown in Fig. 7. An increase in nanoparticle volume fractions reduces the fluid temperature in the channel, which is the result of improved thermal conductivity of the nanofluid. In region 2, conductive heat transfer is prevalent, as shown in Fig. 8.

Dimensionless velocity and temperature distributions for different external power factors are shown in Figs. 9 and 10, respectively. Negative external power factor values increase the intensity of the Lorentz force, which is the active force in this case. As the absolute value of the negative external power factor increases, so does the Lorentz force intensity, which in turn increases the fluid flow velocity in both regions. For K=–0.5, fluid flow is in the direction of the x-axis. For K=0.5, the flow is in the opposite direction of the x-axis. Flow velocities are higher in region 2 than in region 1, except when the K and dimensionless magnetic field velocity values are 0.5; in that case, their influences compensate each other. All these conclusions have been drawn based on the analysis of graphs shown in Fig. 9.

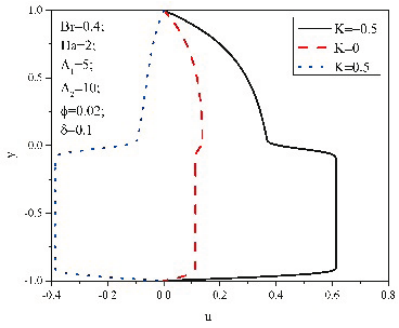

Fig. 9 Velocity distributions for different external electrical load factor (K)

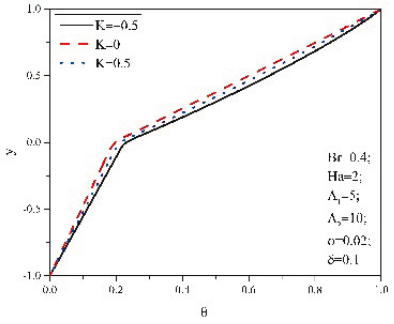

Fig. 10 Temperature distributions for different external electrical load factor (K)

Figure 10 shows that the temperature in the channel is the highest when K=–0.5, and the lowest when K=0.5. This is due to the fact that the Joule heating has the highest value when K=–0.5, and the lowest when K=0.5. This relationship may change if the value of dimensionless magnetic field velocity is different. When K=–0.5, conductive heat transfer is prevalent in region 2 and convective heat transfer in region 1; for the other two K values given here, heat transfer is mostly conductive in both regions.

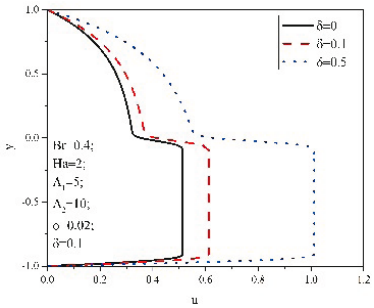

Fig. 11 Velocity distributions for different velocity ratios (δ)

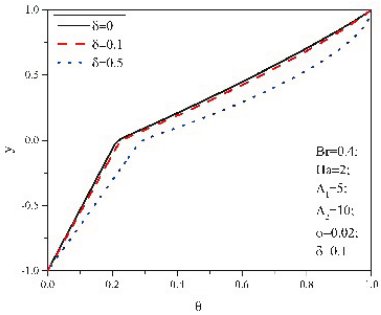

Fig. 12 Temperature distributions for different velocity ratios (δ)

Figures 11 and 12 show dimensionless velocity and temperature distributions for different dimensionless magnetic field velocities, respectively. The distributions shown in Figs. 11 and 12 are given for the external power factor K of –1. A change in the external magnetic field

velocity also changes the Lorentz force intensity. If the external magnetic field moves in the direction of primary fluid flow, then its increase in velocity also increases the active portion of the Lorentz force, but if the magnetic field moves against the primary flow, then its velocity increase intensifies the reactive portion of the Lorentz force. This indicates that the increase in the external magnetic field velocity in the direction of the x-axis causes an increase in the velocity of the fluids in both regions, as shown in Fig. 11. Figure 12 shows that the increase in the dimensionless velocity of the external magnetic field in the direction of the primary flow increases the temperature of fluids in the channel. This in turn causes an increase in the Joule heating, and since it also accelerates fluid flow in the channel, there is an increase in the energy for overcoming the force of Darcy flow resistance; this energy is also transformed into thermal energy. The generated heat raises the fluid temperature in the channel. Conductive heat transfer is prevalent in region 2 and convective heat transfer in region 1. When the value of the external power factor is 0.5, heat is transferred from the fluid to the wall on the top channel wall.

Table 2 provides the numerical values of dimensionless skin friction and the local Nusselt number on the channel walls. As the Hartmann number increases, so does the skin friction on both channel walls. The maximum tangential stress values occur for the highest given value of the Hartmann number. Increase in the porosity factor in region 1 reduces the skin friction on the bottom channel wall. The volume fraction of nanoparticles increases the value of skin friction on both channel walls. Likewise, an increase in the dimensionless velocity of the external magnetic field increases the skin friction on both channel walls. A change in the value of the external power factor changes the values of skin friction on both channel walls. On both walls, the highest stresses occur when the external power factor is –0.5. In all considered cases, the skin friction values on the top wall are greater than the corresponding skin friction values on the bottom wall.

Table 2 Values of skin friction and the Nusselt number for Br=0.4, Ha=2, Λ_1=5, Λ_2=10, ϕ=0.02, K=–0.5, δ=0.1 with the exception of the varying factor

	τ_1	τ_2	Nu_1	Nu_2
Ha=1	–0.657317739	0.1317100	0.697437559	0.938787025
Ha=2	–1.137383097	0.2479316	0.517790748	1.036159793
Ha=3	–1.712762318	0.3675931	0.315749635	1.125134163
Λ_1=5	–1.137383097	0.247931668	0.517790748	1.036159793
Λ_1=10	–0.914268486	0.247931668	0.505921553	1.076001862
Λ_1=15	–0.783910183	0.247931668	0.497762753	1.096362738
ϕ=0	–1.136951475	0.234972796	0.507057706	1.02166939
ϕ=0.01	–1.137164984	0.241363955	0.512500983	1.028961774
ϕ=0.02	–1.137383097	0.247931668	0.517790748	1.036159793
Λ_2=1	–1.137387343	0.247961823	0.518042334	1.033721602
Λ_2=100	–1.137340705	0.24763072	0.515281584	1.060476935
Λ_2=200	–1.137293753	0.247297615	0.512507807	1.087358607
K=–0.5	–1.137383097	0.247931668	0.517790748	1.036159793
K=0	–0.463391946	0.045653941	0.786887713	0.834078733
K=0.5	0.210599205	–0.156623785	0.683412476	0.932536935
δ=0	–1.002584867	0.207476123	0.601415918	0.97170044
δ=0.1	–1.137383097	0.247931668	0.517790748	1.03615979
δ=0.5	–1.676576018	0.409753849	0.034261191	1.41421291

The Nusselt number decreases on the top wall and increases on the bottom wall, i.e., heat transfer velocity decreases on the top wall and increases on the bottom wall when the Hartmann number and porosity factor values increase. An increase in the nanoparticle volume fraction increases heat transfer velocities on both channel walls. An increase in the dimensionless velocity of the external magnetic field reduces the Nusselt number on the top channel wall and increases it on the bottom wall. Changes in external power factor values have an impact on the Nusselt number on both channel walls. The highest Nusselt number value on the top wall occurs when K=0 and on the bottom wall when K=–0.5. In all considered cases, heat transfer velocities on the top wall are lower than the corresponding velocities on the bottom wall.

5. Conclusion

This paper investigated the problem of mixed electromagnetohydrodynamic convection of two immiscible fluids in a horizontal channel. The top and bottom halves of the channel were saturated with different/the same porous media. The top half of the channel contained a pure fluid, and the bottom half contained a nanofluid. The channel was under the influence of an external electric field and an external moving magnetic field. Fluid velocity and temperature distributions were determined analytically and also represented graphically for multiple values of the introduced physical parameters. In addition, the Nusselt number and skin friction values on the channel walls were determined and given in a table for multiple values of the introduced parameters.

Several conclusions were drawn based on the analysis of obtained results, and they are presented below.

- An increase in the Hartmann number accelerates fluid flow in region 1, decelerates it in region 2, and increases the temperature in the channel. At the same time, it increases skin friction on both channel walls, reduces the Nusselt number on the top wall, and increases it on the bottom wall.
- The porosity factor has the same impact as the Hartmann number but does not change the velocity in region 2.
- An increase in the nanoparticle volume fraction decelerates the flow in region 2, minimally changes the velocity in region 1, and decreases the temperature in the channel, while simultaneously increasing skin friction and the Nusselt numbers on both channel walls.
- Higher absolute values of the external power factor are associated with higher fluid velocities in the channel, and when the sign of the power factor changes, the velocity direction also changes. The temperature in the channel is the highest when the external power factor is –0.5.
- Positive/negative values of the dimensionless external magnetic field velocity increase/decrease fluid velocity in the channel. Higher positive values of magnetic field velocity are associated with higher temperatures in the channel and higher skin friction values on both channel walls and lower/higher values of the Nusselt number on the top/bottom wall.

REFERENCES

[1] Choi S.U.S., 1995, *Enhancing thermal conductivity of fluids with nanoparticles*, ASME Int.Mech.Eng. 66, pp. 99-105.

[2] Maxweel J., 1873, *A Treatise on electricity and magnetism*, Publishers to the University of Oxford, at the Clarendon Press.

[3] Goncalves I., Souza R., Goutinho G., Miranda J., Moita A., Pereira J. E., Moreira A., Lima R., 2021, *Thermal Conductivity of Nanofluids: A Review on Prediction Models, Controversies and Challenges*, Applied sciences, 11, 2525, https://doi.org/10.3390/app11062525

[4] Eyad M. Hamad, Aseel Khaffaf, Omar Yasin, Ziad Abu El-Rub, Samer Al-Gharabli, Wael Al-Kouz and Ali J. Chamkha, 2021, *Review of Nanofluids and Their Biomedical Applications, Journal of Nanofluids*, Vol.10, pp. 463-477, https://doi.org/10.1166/jon.2021.1806

[5] D. Nikodjević, Ž. Stamenković, D. Milenković, B. Blagojević, J. Nikodijević, 2011, *Flow and Heat Transfer of Two Immiscible Fluids in the Presence of Uniform Inclined Magnetic Field*, Mathematical Problems in Engineering, Volume 2011, Article ID132302, 18 paages, https://doi.org/10.1155/2011/132302

[6] S. Das, R.N. Jana, O.D. Makinde, 2015, *Mixed convective magnetohydrodinamic flow in a vertical channel filled with nanofluids*, Engineering Science and Technology, an International Journal, https://doi.org/10.1016/j.jestch.2014.12.009

[7] J.A. Lima, G.E. Assad, H.S. Paiva, 2016, *A simple approach to analyze the fully developed two-phase magnetoconvection type flows in inclined parallel-plate channels*, Latin American Applied Research, 46(3). pp. 93-98, https://doi.org/10.52292/j.laar.2016.333

[8] J. Petrović, Ž. Stamenković, M. Kocić, M. Nikodijević, 2016, *„Porous medium magnetohydrodinamic flow and heat transfer of two immiscible fluids“*, Thermal Science, Vol. 20, Suppl. 5, S1405-S1417, https://doi.org/10.2298/TSCI16S5405P

[9] G.S. Seth, R. Tripathi, M.K. Mishra, 2017, *Hydromagnetic thin film flow of Casson fluid in non-Darcy porous medium with Joule dissipation and Navier's partial slip*, Applied Mathematics and Mechanics – English Edition, 38(11), pp. 1613-1626, https://doi.org/10.1007/s10483-017-2272-7

[10] A. S. Dogonchi, M. A. Sheremet, D.D. Ganji, I. Pop, 2019, *Free convection of copper-water nanofluid in a porous gap between hot rectangular cylinder and cold circular cylinder under the effect of inclined magnetic field,* Journal of Thermal Analysis and Calorimetry 135, pp. 1171-1184, https://doi.org/10.1007/s10973-018-7396-3

[11] M. Karuna Prasad, J. Prathap Kumara, J.C. Umavathi, 2019, *Effect of Baffle on Mixed Convection Flow in a Vertical Channel Filled With Electrically Conducting Fluid,* Journal of Engineering Research and Application, Vol.9. Issue 3 (series-V), pp. 12-40; https://doi.org/10.9790/9622-0904011240

[12] Manjeet Mukesh Kumar Sharma, 2020, *MHD flow and heat convection in a channel filled with two immiscible newtonian and nanofluid fluids,* JP Journal of Heat and Mass Transfer, Volume 21, Number 1, pp. 1-21; https://doi.org/10.17654/HM021010001

[13] J.C. Umavathi, Ali J. Chamkha, 2020, *Thermo-Solutal Convection of a Nanofluid Utilizing Fourier's – Type Compass Conditions, Journal of Nanofluids*, Vol.9, pp. 362-374; https://doi.org/10.1166/jon.2020.1759

[14] Milica Nikodijević, Živojin Stamenković, Jelena Petrović, Miloš Kocić, 2020, *"Unsteady fluid flow and heat transfer through a porous medium in a horizontal channel with an inclined magnetic field"*, Transactions of Famena, Vol.44, No.4, pp. 31–46, https://doi.org/10.21278/TOF.444014420

[15] J.C. Umavathi, M.A. Sheremet, 2020, *Heat transfer of viscous fluid in a vertical channel sandwiched between fluids in a porous zones*, Journal of Thermal Analysis and Colorimetry 144(4), https://doi.org/10.1007/s10973-020-09664-1

[16] U.S. Mahabaleshwar, T. Anusha, M. Hatami, 2021, *The MHD Newtonian hybrid nanofluid flow and mass transfer analysis due to super-linear stretching sheet embedded in porous medium*, Scientific reports 11:22518, https://doi.org/10.1038/s41598-021-01902-2

[17] Ankush Raje, Devakar M., Ramgopal N. Ch, 2021, *Influence of heat transfer on the flow of immiscible fluids trough pipes: An analytical study*, Journal of Porous Media 24(11), pp. 85-99, https://doi.org/10.1615/JporMedia.2021038495

[18] Das S., Banu A.S., Jana R.N., Makinde O.D., 2022, *Hall Current's Impact on Ionized Ethylene Glycol Containing Metal Nanoparticles Flowing Through Vertical Permeable Channel*, Journal of Nanofluids, Vol. 11, No. 3, pp. 453-467, https://doi.org/10.1166/jon.2022.1842

[19] Ankush Raje, Ashlesha A. Bhise, 2022, *Heat transport in a sandwiched set-up of MHD Newtonian-Casson-Newtonian fluids trough a porous medium*, Wiley, Heat Transfer, pp. 1-22, https://doi.org/10.1002/htj.22688

[20] J.C. Umavathi, K. Vajraveln, O. Anwar Beg, Umar F. Khan, 2022, *Unsteady squeezing flow of a magnetized dissipative non-Newtonian nanofluid with radiative heat transfer and Fourier-type boundary conditions: numerical study,* Archive of Applied Mechanics, 92, Issue 9, pp. 2695-271, https://doi.org/10.1007/s00419-022-02211-4

[21] T. Linga Raju, B. Venkata Rao, 2022, *The Hall Effect on MHD 2-fluid unsteady heat transfer flow of plasma in a rotating system via a straight channel between conducting plates*, Int. J. of Applied Mechanics and Engineering, Vol. 27, No. 3, pp. 137-162, https://doi.org/10.2478/ijame-2022-0041

[22] M. Karuna Prasad, B.V. Raghu Vamshi Krishna, C.S.K. Raju and Ali J. Chamkha, 2022, *Analytical Study on Magnetohydrodinamic Nanofluid Flow Influenced by Electrical Condusctivity in a Baffled Vertical Channel*, Journal of Nanofluids, Vol. 11, pp. 425-433, https://doi.org/10.1166/jon.2022.1851

[23] T. Linga Raju, B. Venkata Rao, 2022, *Unsteady electro-magneto hydrodinamic flow and heat transfer of two ionized fluids in a rotating system with Hall currents*, Int J. of Applied Mechanics and Engineering, Vol. 27, No. 1, pp. 125-145, https://doi.org/10.2478/ijame-2022-0009

[24] Feroz Ahmed Soomro, Muhammad Usman, Shreen El-Sapa, Muhammad Hamid, Rizwan Ul Haq, 2022, *Numerical study of heat transfer performance of MHD Al2O3-Cu/water hybrid nanofluid flow over inclined surface*, Archive of Applied Mechanics 92, Issue 9, pp. 2757-2765, https://doi.org/10.1007/S00419-022-02214-1

[25] Pramod Kumar Yadav, Ankit Kumar, Shreen El-Sapa, Ali J. Chamkha, 2022, *Impact of thermal radiation and oriented magnetic field on the flow of two immiscible waves in random and complex media*, https://doi.org/10.1080/17455030.2022.2118897

[26] Bullo Hindebu Rikitu, O.D. Makinde, Lemi Guta Enyadene, 2022, *Unsteady mixed convection of a radiating and reacting nanofluid with variable properties, in a porous medium microchannel*, https://doi.org/10.1007/s00419-021-02043-8

[27] Thota Siva, Srinivas Jangili, Bidyasagar Kumbhakar, Pranab Kumar Mondal, 2022, *Unsteady electromagnetohydrodinamic flow of couple stress fluid trough a microchannel: A theoretical analisis*, Europen Journal of Mechanics-B/Fluids, Vol. 95, pp. 83-93, https://doi.org/10.1016/j.euromechflu.2022.04.007

[28] Abdullah K. Alzahrani, Z. Abbas, Malik Zaka Ullah, (2022), Chemically reactive two-phase floww of Alexandria Engineering Journal, https://doi.org/10.1016/j.aej.2022.07.036

[29] Syed Modassir Hussain, Manas Ranjan Mishra, Gauri Shanker Seth, Ali J. Chamkha, 2022, *Dynamics of heat absorbing and radiative hydromagnetic nanofluids though a stretching surface with chemical reaction and viscous dissipation*, ARCHIVE Proceedings of the institution of Mechanical Engineers Part E Journal of Process Mechanical Engineering, pp 1989-1996, https://doi.org/10.1177/09544089221096103

[30] Jelena Petrović, Živojin Stamenković, Jasmina Bogdanović-Jovanović, Milica Nikodijević, Miloš Kocić, Dragiša Nikodijević, 2022, *Electro-Magnetoconvection of Conductive Immiscible Pure Fluid and Nanofluid,* Transactions of FAMENA, Vol. 46 No. 3, pp. 13-28, https://doi.org/10.21278/TOF.463036021

[31] Nabwey, H.A.; Armaghani, T.; Azizimehr, B.; Rashad, A.M.; Chamkha, A.J. (2023), A Compehensive Review of Nanofluid Heat Transfer in Porous Media. Nanomaterials 2023, 13, 937. doi.org/10.3390/nano13050937

[32] P.V. Ananth Subray, B.N. Hannmagowda, C.S.K. Raju, S.V.K. Varma, Prakash Jagdish, Se-Jin Yook, Nehad Ali Shah, (2023), Analytical analysis of inclined three-layered composite channel with cobalt ferrite nanoparticles and Hall current in Darcy medium, Propulsion and Power Research 2023, 12 (4), 523-538, https://doi.org/10.1016/j.jppr.2023.11.001

[33] Shreedevi Kalyan, Hussein Abd Allah Soliman, (2024), Analysis of Micropolar Immiscible Fluid Flow on Electrically Conducting Free Convective Flow in a Vertical Channel in the Presence of Chemical Reaction, International Journal of Advanced Engineering and Business Sciences, Volume 5, Issue 1, pp. 63-90, https://doi.org/10.21608/ijaebs.2024.273140.1093

[34] Rao, S., Deka, P.N., (2024), Numerical Analysiis od MHD Hybrid Nanofluid Flow a Porous Stretching Sheet with Thermal Radiation. Int. J. Appl. Comput. Math 10, 95 (2024). https://doi.org/10.1007/s40819-024-01734-4

[35] I.M. Kirko, G.E. Kirko, 2009, *Magnetic hydrodynamic, Contemporary view of the problem*, Moscow, Izevsk.

[36] Lohrasbi J., Sahani V., 1988, *Magnetohydrodynamic heat and transfer in two-phase flow between parallel plates*, Applied Scientific Research, 45(1), pp. 53-66, https://doi.org/10.1007/BF00384182

[37] M. S. Malashetty, J.C. Umavathi, J. Prathap Kumar, 2001, *Two-fluid Magnetoconvection flow in an inclined channel*, I. J. Trans. Phenomena, Vol. 3, pp. 73-84.

Submitted: 30.9.2024

Accepted: 18.11.2024

Milica Nikodijević Đorđević(CA)*
Faculty of Occupational Safety, Niš, Serbia
Orcid number 0000-0002-6031-1666

Jelena Petrović
Faculty of Mechanical Engineering, Niš, Serbia
jelena.nikodijevic.petrovic@masfak.ni.ac.rs
Orcid number 0000-0001-6768-9779

Živojin Stamenković
Faculty of Mechanical Engineering, Niš, Serbia
zivojin.stamenkovic@masfak.ni.ac.rs

Miloš Kocić
Faculty of Mechanical Engineering, Niš, Serbia
milos.kocic@masfak.ni.ac.rs

Dragiša Nikodijević
Faculty of Mechanical Engineering, Niš, Serbia
dragisan@masfak.ni.ac.rs
Orcid number 0000-0002-1357-6506

*Corresponding author:
milica.nikodijevic@znrfak.ni.ac.rs